Multiferroic phase of doped delafossite $CuFeO_2$ identified using inelastic neutron scattering

Jason T. Haraldsen,[1] Feng Ye,[2] Randy S. Fishman,[1] Jaime A. Fernandez-Baca,[2,3] Yasuhiro Yamaguchi,[4] Kenta Kimura,[4] and Tsuyoshi Kimura[4]

[1]*Materials Science and Technology Division, Oak Ridge National Laboratory, Oak Ridge, Tennessee 37831, USA*

[2]*Neutron Scattering Science Division, Oak Ridge National Laboratory, Oak Ridge, Tennessee 37831, USA*

[3]*Department of Physics and Astronomy, The University of Tennessee, Knoxville, Tennessee 37996, USA*

[4]*Division of Materials Physics, Graduate School of Engineering Science, Osaka University, Osaka 560-8531, Japan*

We report inelastic neutron scattering measurements that provide a distinct dynamical "fingerprint" for the multiferroic ground state of 3.5% Ga-doped $CuFeO_2$. The complex ground state is stabilized by the displacement of the oxygen atoms, which contribute to the multiferroic coupling predicted in the "spin-driven" model. By comparing the observed and calculated spectrum of spin excitations, we conclude that the magnetic ground state is a distorted screw-type spin configuration with a distribution of turn angles.

Multiferroic materials allow the electric polarization to be controlled by switching the direction of magnetic ordering and consequently offer prospects for many technological applications.[1–5] Because multiferroic behavior has been found in materials that exhibit complex (noncollinear and incommensurate) magnetic order, determining the spin arrangement of the ground states is essential to understand its role in the multiferroic coupling.[5–10] In the spin-current model or inverse Dzyaloshinskii-Moriya mechanism of multiferroelectricity,[6–8] the electric polarization is induced by inversion symmetry breaking associated with a complex spin spiral structure. This model predicts that the electric polarization is perpendicular to both the chiral axis $\mathbf{S}_i \times \mathbf{S}_j$ and the magnetic ordering wave vector $\mathbf{Q}$. However, in materials like $CuFeO_2$ and its doped counterparts, the electric polarization is parallel[10–13] to $\mathbf{Q}$, indicating that the spin-current model cannot explain the multiferroic coupling. This multiferroic behavior may instead be explained by spin-orbit coupling with lowered crystal symmetry,[9] which is associated with a lattice distortion in $CuFeO_2$. Therefore, it is important to understand how lattice distortions affect the magnetic structure of these materials.

Nakajima *et al.*[13] proposed that the magnetic structure of multiferroic $CuFeO_2$ is a "proper" spiral configuration composed of two alternating simple spiral structures. Fishman and Okamoto,[14] on the other hand, reported that the ground state for a frustrated triangular lattice has a complex noncollinear (CNC) spin configuration characterized by the presence of higher spin harmonics. Elastic neutron scattering measurements alone are not sufficient to distinguish between these two complex magnetic states because they produce similar sets of observable satellite reflections. Consequently, novel ways must be devised to determine the true magnetic ground state. This Rapid Communication reports inelastic neutron scattering (INS) measurements that provide a distinct dynamical "fingerprint" for the multiferroic ground state of 3.5% Ga-doped $CuFeO_2$. From our analysis, we conclude that the magnetic ground state is a distorted screw-type spin configuration that is incompatible with the generally accepted spin-current model. This complex ground state is stabilized by the displacement of the oxygen atoms, which are also responsible for the multiferroic coupling predicted by Arima.[9]

With a large $S=5/2$ magnetic moment contributed by the Fe^{3+} ions, $CuFeO_2$ [Fig. 1(a)] has inspired great interest due to the magnetic frustration within each hexagonal plane,[15] which results in a $\uparrow\uparrow\downarrow\downarrow$ collinear spin configuration characterized by the propagation wave vector [0.25,0.25,1.5]. A multiferroic state can be induced in this system by applying a magnetic field above about 7 T (Ref. 16) or by doping with nonmagnetic Al or Ga impurities.[11,12] The resulting multiferroic ground state is noncollinear and characterized by the incommensurate propagation wave vectors $Q=[H,H,1.5]$, where $H \approx 0.20$ and 0.30.[17,18] It is notable that the spin excitation spectrum of the collinear nonmultiferroic phase of pure $CuFeO_2$ softens at the incommensurate wave vectors characteristic of the multiferroic phase.[15] This softening can be simulated by lowering the anisotropy energy[19] and the complete softening of this mode signals the development of the multiferroic noncollinear spin structure.[20,21] The observed softening of the spin excitations of $CuFeO_2$ can be interpreted as a dynamical precursor of the multiferroic phase.

Determining the spin configuration of multiferroic $CuFeO_2$ is nontrivial. A simple spiral structure, in which the average turn angle of Fe spins is 74°, would produce the observed peak at [0.20,0.20,1.5] but not the peak at [0.30,0.30,1.5]. Nakajima *et al.*[13] proposed a "proper" spiral configuration [Figs. 1(c) and 1(d)] with two alternating turn angles of 0° and 152° that will produce the two main observed peaks [$H,H,1.5$] ($H \approx 0.20$ and 0.30).

Recently, several groups have observed lattices distortions associated with displacements of the oxygen atoms [illustrated in Fig. 1(b)].[22,23] Incorporating these distortions, Fishman and Okamoto[14] found that odd-order spin harmonics produce a magnetic ground state with a CNC spin configuration [Figs. 1(e) and 1(f)]. The oxygen displacements produce a modulation in the nearest-neighbor interactions J_1 [Fig. 1(b)] that breaks the equilateral symmetry [Fig. 1(b)] of the lattice with nearest-neighbor exchange interactions
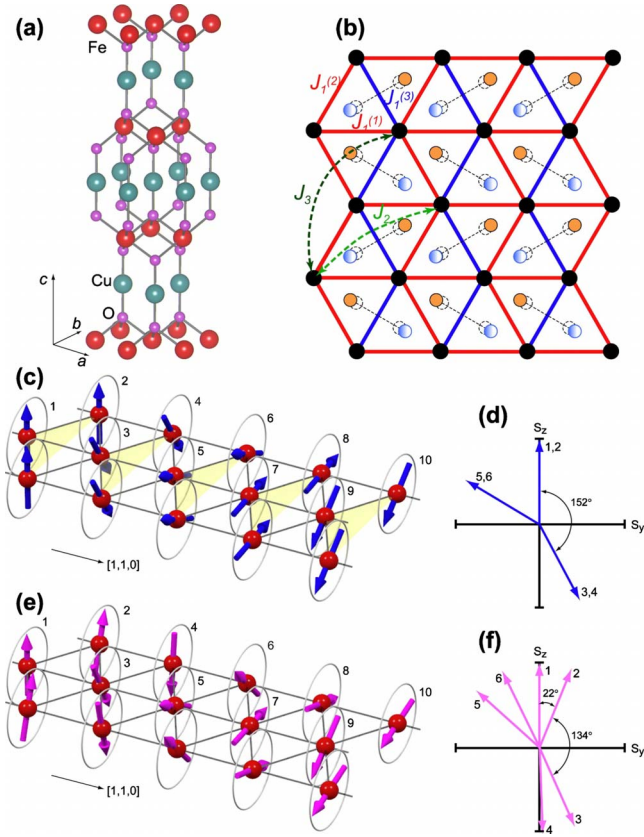
FIG. 1. (Color online) (a) The three-dimensional crystal structure of $CuFeO_2$. (b) The two-dimensional hexagonal lattice structure of the Fe^{3+} layers and the intralayer interactions. The orange (gray) and blue (gray/white) colored atoms illustrate the displacements of oxygen atoms lying above and below the hexagonal plane. The magnetic structure and yz projections of the [(c) and (d)] proper and [(e) and (f)] CNC spiral or screw-type spin configurations are also shown.

$J_1^{(1)} = J_1^{(2)} = J_1 - K_1/2$ and $J_1^{(3)} = J_1 + K_1$, where K_1 is a measure of the atomic distortion. The distortion creates turn angles that fluctuate around $22°$ and $134°$. For a distorted antiferromagnet, a CNC screw-type configuration is energetically favored over both simple and proper spirals.[14] Elastic neutron scattering measurements cannot distinguish between the proper spiral and CNC configurations.

The hexagonal lattice symmetry of $CuFeO_2$ provides a complex network of multiple intralayer and interlayer super-exchange pathways [Fig. 1(b)].[24] The Heisenberg Hamiltonian can be written as

$$H = -\frac{1}{2}\sum_{i \neq j} J_{ij}\mathbf{S}_i \cdot \mathbf{S}_j - D\sum_i \mathbf{S}_{iz}^2, \qquad (1)$$

where $\mathbf{S}_i$ is the local moment on site i, D is the anisotropy energy, and the exchange coupling J_{ij} between sites i and j is antiferromagnetic when $J_{ij} < 0$.

To incorporate the spin harmonics, we modified the classical approach described in Ref. 14 by defining S_z within any hexagonal plane as

$$S_z(\mathbf{R}) = A\left\{\sum_{l=0} C_{2l+1}\cos[Q(2l+1)x] - \sum_{l=0} B_{2l+1}\sin[(2\pi - Q)(2l+1)x]\right\}, \qquad (2)$$

where the C_{2l+1} harmonics are produced by the anisotropy energy D and the B_{2l+1} harmonics are produced by the lattice distortion K_1. The square of these harmonics are proportional to the observed elastic intensities at odd multiples of Q and $2\pi - Q$. In the function $S_z(\mathbf{R})$, A is normalized so that the maximum of $|S_z(\mathbf{R})|$ is $S = 5/2$. The perpendicular spin S_y is given by

$$S_y(\mathbf{R}) = \sqrt{S - S_z(\mathbf{R})^2}\,\text{sgn}[g(\mathbf{R})], \qquad (3)$$

where

$$g(\mathbf{R}) = \sin(Qx) + G_1\cos[(2\pi - Q)x] \qquad (4)$$

and G_1 is an additional variational parameter.

Hexagonal spin planes were then stacked along the c axis and coupled by the exchange interactions J_{zn}. The three-dimensional spin configuration was obtained by minimizing the energy on a large unit cell with length 10^4. The spin fluctuations about this three-dimensional spin configuration were evaluated using the method described in Ref. 25, where the frequencies and intensities of the spherical wave (SW) excitations are evaluated simultaneously. We emphasize that a stable ground state is required to evaluate the spin dynamics: a $1/S$ spin-wave expansion cannot be performed starting from the proper helix sketched in Fig. 1(c).

Single crystals of $CuFe_{0.965}Ga_{0.035}O_2$ were grown using the floating-zone technique. The crystals were oriented with two orthogonal wave vectors of $[1,1,0]$ and $[0,0,3]$ aligning in the horizontal plane. The INS measurements were carried out using the cold neutron chopper spectrometer (CNCS) spectrometer at the Spallation Neutron Source (SNS) and the HB-1 triple-axis spectrometers at the High Flux Isotope Reactor (HFIR) at the Oak Ridge National Laboratory. The low energy excitations were measured at 1.4 K with final energy chosen at 5.1 meV at HB-1 and with incident neutron energy chosen at 3 meV to ensure high resolution at CNCS.

Figures 2(a) and 2(b) present the INS data for the multiferroic phase of 3.5% Ga-doped $CuFeO_2$ along $[H,H,0]$ with $L = 1.5$. "Gapless" excitations are observed at $H \approx 0.20$ and 0.30 together with a "shoulder" at $H \approx 0.08$ and an intensity "hole" around $H \approx 0.30$ and $E \approx 1.0$ meV. Using the interactions presented in Table I, Fig. 2(c) displays the predicted INS spectra,[26] which contains contributions from both the normal spin configuration with wave vector along $[H,H,1.5]$ and the two twins with wave vectors along $[H,0,1.5]$ and $[0,H,1.5]$. Strongly affected by the lattice distortion, the twin states account for the spectral weight around $E \approx 1.5$ meV and $H \approx 0.30$. The model also accurately produces the intensity "hole" at $H \approx 0.30$ as well as the shoulder at $H \approx 0.08$, which is caused by the interlayer interactions. With the number of intricate features reproduced, we are confident that the dynamical fingerprint of doped $CuFeO_2$ has been matched.
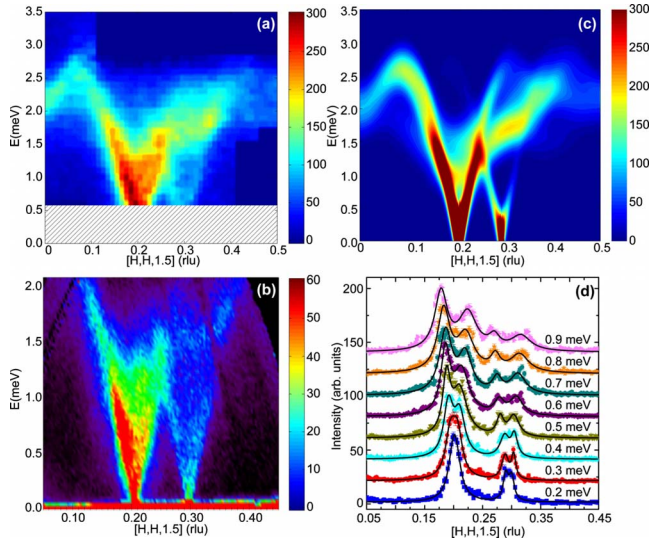
FIG. 2. (Color online) Energy versus momentum transfer taken from (a) the triple-axis spectrometer at HFIR and (b) the time-of-flight CNCS at the SNS. (c) Predicted simulation of the INS data using intralayer and interlayer interactions along with a lattice distortion and anisotropy. (d) Wave vector scans with different energy transfers for the CNCS data.

To compare the experimental and theoretical results more closely, we examined the SW velocities $d\omega/dq$ at low energy [Fig. 4(b)]. The data points are determined by the energy cuts plotted in Fig. 2(d). Since the SW velocities are functions of the exchange interactions, this comparison assures us that the correct exchange parameters have been used. As shown in Table I, the exchange parameters J_n and J_{zn} are quite close[26] to those predicted in Ref. 24 from fits to the SW spectra of the $\uparrow\uparrow\downarrow\downarrow$ phase. The experimental results show no evidence of an energy gap present in the multiferroic phase within the experimental energy resolution. This is consistent with our model, in which rotations of the spin plane about the c axis cost no energy and a SW gap is absent. However, the magnetostrictive energy that produces the observed confinement[13] of the spins to the [1,1,0] plane may induce a small gap in the excitation spectrum.

While four harmonics are predicted, only the B_1 component produces sufficient scattering intensity comparing to the main mode at [0.20,0.20,1.5] to be seen by our INS measurements.[26] While the main SW mode is associated with the ordering wave vector Q, the secondary mode centering at [0.30,0.30,1.5] is produced by the B_1 harmonic at $2\pi-Q$. The overall magnitudes of these modes are in agreement with our calculated values. For lower Ga doping or larger anisotropy, the higher harmonics will become more important and the distribution of turn angles will become more uniformly distributed. If D is increased from 0.01 to 0.04 meV (the critical value above which the $\uparrow\uparrow\downarrow\downarrow$ phase is stable) then the amplitudes C_3 and B_3 rise by factors of 2 and 4, respectively.

Similar to the collinear excitation observed[15] in pure CuFeO$_2$, the dispersive excitation along the [0,0,L] direction through the magnetic Bragg peak at $H\approx0.20$ contains a minimum at $L=1.5$ [Figs. 3(a) and 3(b)]. This underscores
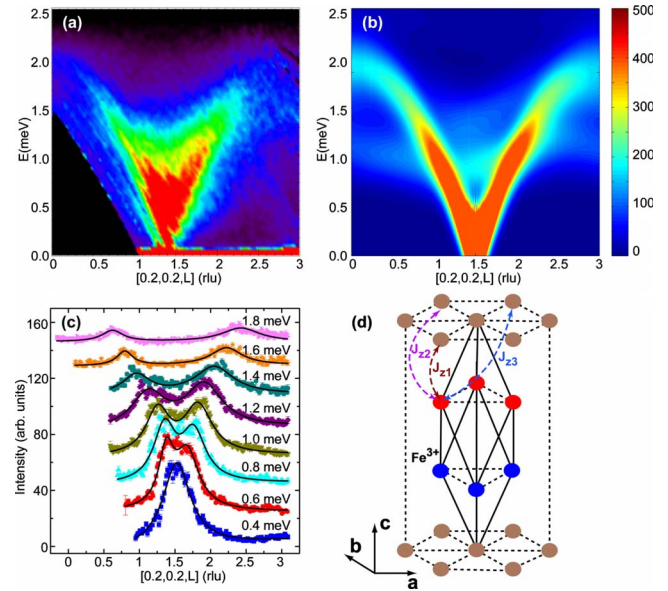

FIG. 3. (Color online) (a) Energy versus momentum transfer taken from the CNCS clearly showing the SW modes along the [0,0,L] direction with $H=0.2$. The dispersion with L indicates the importance of interlayer interactions. (b) Predicted INS spectra using intralayer and interlayer interactions along with a lattice distortion. (c) Intensity versus momentum transfer for various energies. (d) A three-dimensional view of the Fe^{3+} lattice structure illustrating the interlayer interactions.

the importance of the interlayer interactions J_{zn} [Fig. 3(d)] and the three-dimensional character of this system. In comparison to pure CuFeO$_2$, the magnetic interactions J_{z2} and J_{z3} are somewhat weakened,[26] which may be attributed to the disorder caused by Ga doping. Figure 3(c) shows the experimental cuts in energy demonstrating the splitting of the Goldstone mode at $L\approx1.5$.
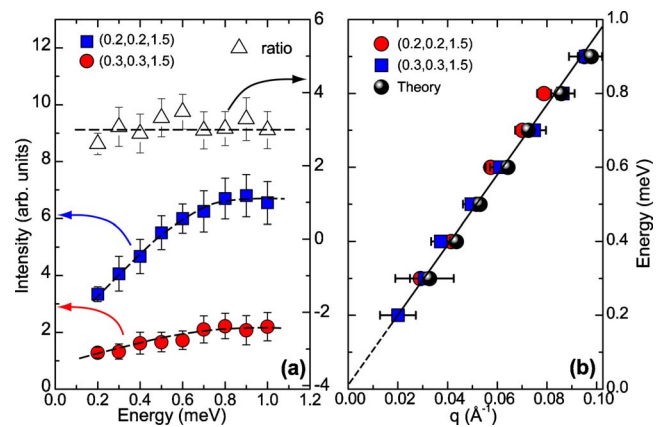

FIG. 4. (Color online) (a) Intensity versus energy for the [0.20,0.20,1.5] (blue/gray squares) and [0.30,0.30,1.5] (red/gray circles) modes along the [H,H,0] direction with $L=1.5$. The ratio of mode intensities (open triangles) shows that the main [0.20,0.20,1.5] mode is three times as intense as the [0.30,0.30,1.5] mode. The simulated intensity is consistent with this intensity ratio. (b) SW velocities for the two modes along the [H,H,0] direction with $L=1.5$ together with the predicted values (black circles).

TABLE I. Hamiltonian parameters (in meV) for $CuFe_{1-x}Ga_xO_2$.

x	J_1	J_2	J_3	J_{z1}	J_{z2}	J_{z3}	D	Ref.
0.000	−0.23	−0.12	−0.16	−0.06	0.07	−0.05	0.22	24
0.035[a]	−0.19	−0.10	−0.13	−0.05	0.02	−0.01	0.01	

[a]Includes a lattice distortion of $K_1 = 0.07$ meV.

Figure 4(a) compares the integrated scattering intensity originating from the main mode at $H = 0.20$ and the secondary mode at $H = 0.30$. The main mode is about three times as intense as the secondary one. The simulation with $B_1 = -0.52$ yields an intensity ratio of 3.7, in good agreement with the measured value. The only well-defined modes in our model are the Goldstone modes emerging from [0.20,0.20,1.5] and [0.30,0.30,1.5]. A continuum of excitations borders the Goldstone modes due to the complex and incommensurate nature of the magnetic structure. This contrasts with the relatively large gapped excitation and associated magnon-phonon hybridized electromagnon observed in $TbMnO_3$.[27]

According to Ref. 9, the spin-driven multiferroic behavior of $CuFeO_2$ arises from the uniform charge transfer through the metalligand hybridization in the presence of spin-orbit coupling. Using a combination of INS measurements and theoretical modeling, we have demonstrated that lattice distortions play an important role in determining the magnetic ground state of Ga-doped $CuFeO_2$. With a slight modification of the exchange parameters from pure $CuFeO_2$ and by adjusting the anisotropy and distortion energies, we have achieved remarkable agreement between the observed and predicted dynamical fingerprint of the CNC multiferroic phase. This complex ground state provides an alternative way to realize multiferroic coupling, where displacements of the oxygen atoms severely distort the spin configuration and produce the electric polarization. Consequently, it is clear that the spin-current model[6–8] is not the only mechanism responsible for multiferroic behavior and that many other frustrated magnets with rhombohedral or hexagonal symmetries may also exhibit the same form of multiferroic coupling as doped $CuFeO_2$.[28,29] The symmetry of these materials makes them candidates for exotic magnetoelectric control like the recently reported magnetic digital flop of ferroelectric domains.[30]

[1] T. Kimura, T. Goto, H. Shintani, K. Ishizaka, T. Arima, and Y. Tokura, Nature (London) **426**, 55 (2003).

[2] D. I. Khomskii, J. Magn. Magn. Mater. **306**, 1 (2006).

[3] S.-W. Cheong and M. Mostovoy, Nature Mater. **6**, 13 (2007).

[4] R. Ramesh and N. A. Spaldin, Nature Mater. **6**, 21 (2007).

[5] W. Eerenstein, N. D. Mathur, and J. F. Scott, Nature (London) **442**, 759 (2006).

[6] H. Katsura, N. Nagaosa, and A. V. Balatsky, Phys. Rev. Lett. **95**, 057205 (2005).

[7] M. Mostovoy, Phys. Rev. Lett. **96**, 067601 (2006).

[8] I. A. Sergienko and E. Dagotto, Phys. Rev. B **73**, 094434 (2006).

[9] T. Arima, J. Phys. Soc. Jpn. **76**, 073702 (2007).

[10] M. Soda, K. Kimura, T. Kimura, M. Matsuura, and K. Hirota, J. Phys. Soc. Jpn. **78**, 124703 (2009).

[11] S. Seki, Y. Yamasaki, Y. Shiomi, S. Iguchi, Y. Onose, and Y. Tokura, Phys. Rev. B **75**, 100403(R) (2007).

[12] S. Kanetsuki, S. Mitsuda, T. Nakajima, D. Anazawa, H. A. Katori, and K. Prokes, J. Phys.: Condens. Matter **19**, 145244 (2007).

[13] T. Nakajima *et al.*, J. Phys. Soc. Jpn. **76**, 043709 (2007).

[14] R. S. Fishman and S. Okamoto, Phys. Rev. B **81**, 020402(R) (2010).

[15] F. Ye, J. A. Fernandez-Baca, R. S. Fishman, Y. Ren, H. J. Kang, Y. Qiu, and T. Kimura, Phys. Rev. Lett. **99**, 157201 (2007).

[16] T. Kimura, J. C. Lashley, and A. P. Ramirez, Phys. Rev. B **73**, 220401(R) (2006).

[17] N. Terada, S. Mitsuda, T. Fujii, K. Soejima, I. Doi, H. A. Katori, and Y. Noda, J. Phys. Soc. Jpn. **74**, 2604 (2005).

[18] N. Terada, T. Nakajima, S. Mitsuda, H. Kitazawa, K. Kaneko, and N. Metoki, Phys. Rev. B **78**, 014101 (2008).

[19] R. S. Fishman, J. Appl. Phys. **103**, 07B109 (2008).

[20] M. Swanson, J. T. Haraldsen, and R. S. Fishman, Phys. Rev. B **79**, 184413 (2009).

[21] J. T. Haraldsen, M. Swanson, G. Alvarez, and R. S. Fishman, Phys. Rev. Lett. **102**, 237204 (2009).

[22] F. Ye, Y. Ren, Q. Huang, J. A. Fernandez-Baca, P. Dai, J. W. Lynn, and T. Kimura, Phys. Rev. B **73**, 220404(R) (2006).

[23] N. Terada, S. Mitsuda, H. Ohsumi, and K. Tajima, J. Phys. Soc. Jpn. **75**, 023602 (2006).

[24] R. S. Fishman, F. Ye, J. A. Fernandez-Baca, J. T. Haraldsen, and T. Kimura, Phys. Rev. B **78**, 140407(R) (2008).

[25] J. T. Haraldsen and R. S. Fishman, J. Phys.: Condens. Matter **21**, 216001 (2009).

[26] The resulting harmonics are $C_3 = -8.4 \times 10^{-4}$, $C_5 = -4.0 \times 10^{-5}$, $B_1 = -0.52$, and $B_3 = -0.011$, which are all normalized with respect to the main contribution $C_1 = 1$. The C_3 and B_3 harmonics produce excitations at wave vectors [0.4,0.4,1.5] and [0.1,0.1,1.5]. Although these features are too weak to be observed in the 3.5% Ga-doped compound, their observation in more weakly doped $CuFeO_2$ should distinguish the CNC phase from the proper spiral in elastic neutron scattering measurements.

[27] D. Senff, P. Link, K. Hradil, A. Hiess, L. P. Regnault, Y. Sidis, N. Aliouane, D. N. Argyriou, and M. Braden, Phys. Rev. Lett. **98**, 137206 (2007).

[28] T. Arima: JPSJ OnlineNews and Comments, December 10, 2009.

[29] M. Poienar *et al.*, Phys. Rev. B **81**, 104411 (2010).

[30] S. Seki, H. Murakawa, Y. Onose, and Y. Tokura, Phys. Rev. Lett. **103**, 237601 (2009).